Author Manuscript

Author Manuscript

Author Manuscript

Author Manuscript

HHS Public Access

Author manuscript

J Am Soc Mass Spectrom. Author manuscript; available in PMC 2024 January 04.

Published in final edited form as:

J Am Soc Mass Spectrom. 2023 January 04; 34(1): 82–91. doi:10.1021/jasms.2c00262.

Diethylpyrocarbonate-based Covalent Labeling Mass Spectrometry of Protein Interactions in a Membrane Complex System

Xiao Pan[1], **Thomas Tran**[2], **Zachary J. Kirsch**[1], **Lynmarie K. Thompson**[1,2], **Richard W. Vachet**[1,2,*]

[1]Department of Chemistry, University of Massachusetts Amherst, Amherst, MA 01003

[2]Molecular and Cellular Biology Program, University of Massachusetts Amherst, Amherst, MA 01003

Abstract

Membrane-associated proteins are important because they mediate interactions between a cell's external and internal environment and they are often targets of therapeutics. Characterizing their structures and binding interactions, however, is challenging because they typically must be solubilized using artificial membrane systems that can make measurements difficult. Mass spectrometry (MS) is emerging as a valuable tool for studying membrane-associated proteins, and covalent labeling MS has unique potential to provide higher order structure and binding information for these proteins in complicated membrane systems. Here, we demonstrate that diethylpyrocarbonate (DEPC) can be effectively used as a labeling reagent to characterize the binding interactions between a membrane-associated protein and its binding partners in an artificial membrane system. Using chemotaxis histidine kinase (CheA) as a model system, we demonstrate that DEPC-based covalent labeling MS can provide structural and binding information about the ternary complex of CheA with two other proteins that is consistent with structural models of this membrane-associated chemoreceptor system. Despite the moderate hydrophobicity of DEPC, we find that its reactivity with proteins is not substantially influenced by the presence of the artificial membranes. However, correct structural information for this multi-protein chemoreceptor system requires measurements of DEPC labeling at multiple reagent concentrations to enable an accurate comparison between CheA and its ternary complex in the chemoreceptor system. In addition to providing structural information that is consistent with the model of this complex system, the labeling data supplements structural information that is not sufficiently refined in the chemoreceptor model.

Graphical Abstract

[*]**Corresponding Author**: rwvachet@chem.umass.edu; Phone: (413) 545-2733 (R.W.V.).

Supporting Information

Additional information, including DEPC labeling data of CheA with and without vesicles, the DEPC concentration-dependent reactivity of the 20 residues studied here, and additional views of the chemoreceptor complex structural models, can be found in the Supporting Information section. The Supporting Information is available free of charge on the ACS Publications website at DOI:

The authors declare no competing financial interest.

Author Manuscript Author Manuscript Author Manuscript Author Manuscript

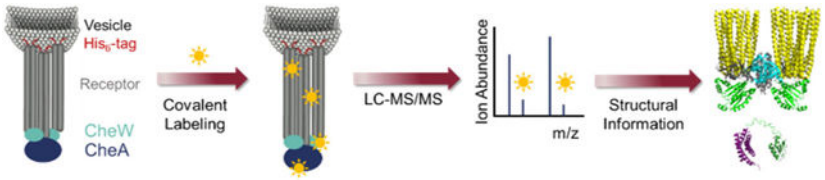

Covalent labeling using diethylpyrocarbonate with mass spectrometric detection is used to successfully identify protein-protein binding sites for CheA in an artificial membrane system.

Introduction

Membrane proteins play important roles in living organisms such as catalysis, cell signaling, cell adhesion, and transport. They also mediate interactions between a cell's external and internal environment. Responses to external stimuli are often controlled via membrane proteins that act as receptors capable of binding with molecules in the extracellular space and transmitting these signal across the cell membrane.[1] G-protein-coupled receptors (GPCRs) are perhaps the best example of membrane protein receptors that mediate cellular responses upon binding to neurotransmitters and hormones.[2] Probing the interactions between membrane proteins like GPCRs and their ligands is essential for understanding and controlling their function. The importance of membrane protein interactions can be further appreciated by the fact that about 60% of the drugs that have been approved by the Food and Drug Administration (FDA) target membrane proteins.[3] Because of their importance in cell function and disease treatments, it is crucial to characterize the higher order structures and binding interactions of membrane proteins. However, in contrast to water-soluble proteins, it is generally challenging due to their flexibility, partially hydrophobic surfaces, and lack of stability.[4] Membrane proteins are often studied in the presence of artificial membrane such as micelles, bicelles, amphipols, or lipid nanodiscs,[5,6] which are necessary to maintain their structures but create technical challenges during analysis.

X-ray crystallography,[7] cryo-electron microscopy (cryo-EM),[8] solution and solid-state nuclear magnetic resonance (NMR),[9] and single-molecule tracking with fluorescence spectroscopy[10–12] are measurement techniques that have been used to characterize membrane protein structure. Each method, however, has its limitations with regards to sample preparation, molecular weight limits, sample purity, or structural resolution. For example, co-crystallization of membrane proteins with artificial membranes is difficult, making X-ray crystallography not broadly applicable. As another example, NMR has protein molecular weight limitations and can be challenging in complex protein mixtures.

Mass spectrometry (MS) is emerging as a valuable tool for studying membrane proteins and their complexes. The advantages of MS are its high sensitivity, moderate structural resolution, relatively high-throughput, and ability to study proteins in complex mixtures.[13] Native MS can be used to provide membrane protein structural information and binding stoichiometries.[14] Ion mobility (IM)-MS, coupled with collision-induced dissociation (CID), collision-induced unfolding (CIU), or surface-induced dissociation (SID) can report protein stoichiometry and architecture information.[15–17] Hydrogen/deuterium exchange (HDX)-MS has been used to monitor membrane protein secondary structure and backbone dynamics

Author Manuscript Author Manuscript Author Manuscript Author Manuscript

via the increase of deuterium uptake on the peptide level over time.[18–20] Chemical cross-linking (XL)-MS can provide information about subunit connectivity of membrane protein complexes and protein interactions using bi-functional reagents that link nearby residues.[21–22]

Covalent labeling (CL)-MS has also recently been used to study membrane protein structure and interactions due to its inherent advantages, such as measurement simplicity, no back-exchange and no label scrambling.[23] In CL-MS, a chemical reagent covalently modifies solvent-exposed residue side chains on a protein or protein complex. The stable modification allows the use of optimized proteomics techniques to facilitate its localization. A variety of residue non-specific reagents (e.g. hydroxyl radicals) and residue-specific reagents (e.g. succinimides for Lys residues) are available.[24–25] Residue specific methods have the advantage of simplicity as compared to residue non-specific approaches. Upon comparing modification percentages of a free protein to a protein with its partner, binding interfaces and conformational changes can be revealed with residue-level resolution.

One CL reagent that is simple to use and has potential for studying membrane protein structure is diethylpyrocarbonate (DEPC). DEPC is a pseudo-specific CL reagent that modifies the side chains of nucleophilic residues such as His, Lys, Tyr, Ser, Thr, Cys, and the N-terminus, providing moderate structural resolution. Two previous studies revealed the promise of DEPC for studying membrane proteins, but the full potential of this reagent for these proteins has not been realized. Schmidt *et al.* used DEPC labeling together with native MS and XL-MS data as modeling constraints to assemble a structural model of F-type ATP synthase in n-dodecyl-β-D-maltoside (DDM) detergent micelles.[26] This work suggested that adequate residue solvent accessibility information can be obtained from DEPC labeling to help narrow down possible structures when combined with other data. However, the ability of DEPC labeling to act as a standalone reagent for studying membrane protein structure and binding interactions was not explored. More recently, Guo *et al.* demonstrated that DEPC can modify the membrane protein vitamin K epoxide reductase in DDM micelles, but they found that labeling occurs not only on extra-membrane regions of the protein but also in transmembrane regions.[27] These researchers, however, found that sonication was necessary to increase labeling yield, which may explain labeling in the transmembrane regions of the protein.

In our work here, we investigate whether DEPC labeling can be used to study binding interactions in a membrane-associated protein complex in an artificial membrane system. DEPC has been found to be exceptionally useful for studying protein-protein interactions,[28–31] but the capability of this reagent to probe such protein-protein interactions in an artificial membrane system has not been shown. DEPC is a somewhat hydrophobic molecule with a calculated logP value of 1.316,[32] an experimentally estimated log P value of 1.10,[33] and a solubility in water of ~ 40 mM.[34] These parameters suggests that DEPC might partition to some extent into the lipid or detergent phase of an artificial membrane system, influencing its reactivity with proteins. To explore DEPC capability as a labeling reagent for membrane protein interactions, we use chemotaxis histidine kinase (CheA) as a model system. CheA is part of a membrane-associated chemoreceptor system that controls the swimming direction of certain bacteria (Figure 1a).[35] The protein consists of

Author Manuscript Author Manuscript Author Manuscript Author Manuscript

five domains (P1 to P5) and is a homodimer in the chemoreceptor complex.[36] The P1 domain has the phosphorylation site (His48); the P2 domain mediates binding to response regulator proteins, CheB and CheY (not present in our studies here); P3 is the dimerization domain; P4 is the catalytic domain; and P5 binds to CheW and transmembrane receptors in the signaling complex, which we study here. When specific attractant molecules bind to the receptor complex, signals are transmitted across the membrane to direct the swimming of the bacteria. No complete crystal or NMR structure exists for this complex, but a structural model has been built for the complex between CheA, CheW and a cytoplasmic fragment of the receptor (pdb 6s1k,[37] Figure 1a). We have assembled such complexes using a cytoplasmic fragment of the *E coli* Asp receptor (CF4Q), mediated by binding of the His-tagged receptor fragment to vesicles bearing metal-chelating head groups (Figure 1b).[38] We are interested in using DEPC CL-MS to study the structural changes and binding interactions of CheA upon interacting with this membrane complex system. These results will provide an indication of the ability of DEPC CL-MS to study membrane protein binding and should provide additional information for the CheA structure in complex, helping to refine the structural model.

Experimental Section

Materials

Human angiotensin II (#A9525), bradykinin (#B3259), diethylpyrocarbonate (DEPC) (#D5758), imidazole (#I5513), iodoacetamide (#I6125), and trypsin from bovine pancreas (#T1426) were all purchased from Sigma-Aldrich (St. Louis, MO). Urea (#424581000) was bought from Acros Organics (Fair Lawn, NJ). Formic acid (#A117), water (#W7), and acetonitrile (#A998) were obtained from Fisher Scientific (Fair Lawn, NJ). Amicon® centrifugal filters (#UFC501096 & #UFC800324) were from Millipore Sigma (Burlington, MA). A kinase buffer (50 mM K_2HPO_4, 5 mM $MgCl_2$, 75 mM KCl, pH 7.5) and large unilamellar vesicles containing 60% 1,2-dioleoylsn-glycero-3-phosphocholine (DOPC) and 40% nickel chelating lipid DGS-Ni^{2+}-NTA (1,2-dioleoyl-*sn*-glycero-3-{[*N*-(5-amino-1-carboxypentyl)-iminodiacetic acid]succinyl}) were prepared using previously described methods.[39] CheA, CheW, and the cytoplasmic fragment (CF4Q) were expressed and purified using previously described methods.[39]

Membrane Complex Assembly and Activity Assays

Functional signaling complexes were prepared by incubating 3 μM CheA, 18 μM CheW, 30 μM CF4Q and 860 μM vesicles in kinase buffer overnight. These assembly conditions maximize the percentage of CheA bound (~90%) in signaling complexes, based on sedimentation assays as previously described.[39] After incubation, the CheA kinase activity was measured using an enzyme-coupled assay that monitors the decrease of NADH absorbance (340 nm) as the result of ATP consumption coupled to NADH oxidation. The reaction was initiated by addition of 2 μL of complex to a CheY mixture that contains 56 μM CheY, 20 units of pyruvate kinase/lactic dehydrogenase enzyme mixture (Sigma), 4 mM ATP (Fisher Scientific), 1.5 mM phosphoenolpyruvate (Sigma), and 200 μM NADH (Sigma). The absorbance was recorded for 1.2 min, and the resulting slope for the complex was corrected by subtracting the slope recorded for a CheY-only control sample. Specific

Author Manuscript Author Manuscript Author Manuscript Author Manuscript

activity per CheA (s^{-1}) was calculated by equation 1. Only assemblies with high CheA activity (> 20 s^{-1}) were labeled by DEPC.

$$Specific\ activity\ per\ CheA\left(s^{-1}\right) = \frac{\left(Adjusted\ slope, \frac{abs}{min}\right) * \left(\frac{1min}{60s}\right) * \left(\frac{200uL}{2uL}\right)}{\left(6220\frac{abs}{M}\right) * [total\ CheA\ in\ complex]} \quad (1)$$

Because unbound CheA from *E. coli* has undetectable kinase activity in our assay, high kinase activity indicates high complex formation. For instance, for a series of five samples with a kinase activity of 20 ± 3 s^{-1}, the fraction of CheA bound was 88 ± 7% from sedimentation assays.

DEPC Labeling Reactions

Bradykinin (51 μM) and angiotensin II (51 μM) were prepared in a kinase buffer at pH 7.5. DEPC labeling of these peptides were conducted without and with vesicles present to quantitatively test the effect of the lipid vesicles on DEPC reactivity. The concentration of vesicles in the samples was 860 μM. DEPC stock solutions were freshly prepared in dehydrated acetonitrile for each experiment. Peptides were reacted with DEPC at 37 °C for 1 min in a total volume of 50 μL at various molar excesses ranging from 2 to 10. The reaction was then quenched by the addition of imidazole at a 1:50 DEPC:imidazole molar ratio.

51 μM CheA or complexes containing 51 μM protein in total (3 μM CheA, 18 μM CheW, 30 μM CF4Q) and 860 μM vesicles were reacted with DEPC at 37 °C for 5 min in a total volume of 50 μL at various molar excesses ranging from 4 to 10. The DEPC concentration was chosen to minimize protein structural perturbations based on predictions from previous work.[40] The DEPC labeling reactions were quenched by imidazole. To prevent protein structural perturbation, the final amount of acetonitrile in the protein solution was kept to < 3% (v/v).

Proteolytic Digestion

After the DEPC reactions were quenched, 8.0 M urea was added to the protein or protein complex sample and incubated for 10 min to unfold the proteins. Iodoacetamide was added in a molar excess of 120 to alkylate the free Cys residues, which is essential for avoiding the DEPC labeling of previously unreacted Cys residues.[41] The samples were kept in the dark at room temperature for 30 min. After that, the samples were desalted and preconcentrated via Amicon® centrifugal filters with a 10 kDa molecular weight cutoff (MWCO) to ensure the concentration of urea was less than 2.0 M. Soluble trypsin was added into the samples at a 1:10 (w/w) enzyme:substrate ratio. The digestion was performed for 16 hours at 37 °C, and finally the enzyme was separated by centrifugal filters with a 3 kDa MWCO.

Liquid Chromatography (LC)

Online LC-MS/MS analyses were performed on a Thermo Scientific Dionex Ultimate 3000 HPLC system (Waltham, MA) with a Thermo Scientific Acclaim™ PepMap™ RSLC C18 column (15 cm × 300 μm, 2 μm particle size, 100 Å pore size) at a flow rate of 4 μL/min. The mobile phases were water and acetonitrile, both containing 0.1% formic acid. For

Author Manuscript Author Manuscript Author Manuscript Author Manuscript

the bradykinin and angiotensin II samples, the mobile phase composition started at 5% acetonitrile for the first 5 min, went to 50% over the next 15 min and then was followed by a flush mobile phase of 95% acetonitrile. For protein digests, the mobile phase started at 5% acetonitrile. After 5 min, it was increased to 50% acetonitrile over 50 min and finally was elevated to and held at 95% to flush the column for 5 min. For samples containing the vesicles, an additional 45-min flush of mobile phase was used to ensure the lipids were removed from the column.

Mass Spectrometry

Mass spectra of bradykinin and angiotensin II were acquired on a Bruker AmaZon quadrupole ion trap (Billerica, MA). The electrospray needle voltage was kept at 4.1 kV with the capillary temperature at 250 °C. To identify the modification sites, collision-induced dissociation (CID) was conducted with a ramp of voltages from 0.9 to 2.7 V. LC-MS of protein digests were acquired on a Thermo Scientific Orbitrap Fusion mass spectrometer (Waltham, MA). The electrospray voltage was 4.0 kV, and the ion transfer tube temperature was 275 °C. The resolution of the orbitrap was set to 60,000, and a 100 ms maximum injection time was used. CID was conducted in the linear quadrupole ion trap with collision energy of 35%. The width of the isolation window was 2.0 Da. Parallel reaction monitoring (PRM) was used to measure the modified peptides from the protein digests. In these experiments the resolution of the orbitrap was set to 30,000 and a 50 ms maximum injection time was used. The precursor ions (unmodified or modified peptide ions) were selected, and CID was performed with collision energy of 35%. Product ions were detected by the orbitrap analyzer with a resolution of 30,000.

Peak Identification and Modification Level Quantification

The extent of modification on a given peptide was calculated as follows (eq. 2).

$$Extent\ of\ Modification = \frac{\sum_{z=1}^{n} x\, Peak\ area_z^{Modified}}{\sum_{z=1}^{n} Peak\ area_z^{Modified} + \sum_{z=1}^{n} Peak\ area_z^{Unmodified}} \quad (2)$$

Where x is the number of modifications on the peptide, z is the peptide charge state, and all charge states of a given peptide are considered. Data processing of results on the Bruker AmaZon was performed using Bruker Compass™ data analysis 4.0.

The percentage of labeling on a given residue was calculated as follows (eq. 3).

$$Percentage\ of\ Labeling = \frac{\sum_{i=1}^{n}\sum_{z=1}^{m} Peak\ \ area_{i,z}^{Modified}}{\sum_{i=1}^{n}\sum_{z=1}^{m} Peak\ \ area_{i,z}^{Modified} + \sum_{i=1}^{n}\sum_{z=1}^{m} Peak\ \ area_{i,z}^{Unmodified}} \times 100 \quad (3)$$

where i represents the residue of interest and z is the charge state. In the calculation shown in equation 3, the signal from all the peptides that contain the modified residue of interest are summed. In PRM, the calculations were based on the peak area of extracted ion chromatograms by choosing the three most abundant b or y ions in the peptide tandem

Author Manuscript Author Manuscript Author Manuscript Author Manuscript

mass spectra. To correct for day-to-day instrument variations, labeling percentage data at a 10-fold molar ratio of DEPC were used to normalize the results at other concentrations. Data processing of results on the Thermo Scientific Orbitrap Fusion was performed using Thermo Xcalibur and a custom software pipeline.[42]

Results and Discussion

DEPC Labeling of CheA in Solution vs. Complex

CL-MS provides information about protein binding interactions and conformational changes by comparing residue modification extents of a free protein to the same protein in a complex. Here, DEPC was used to modify the CheA dimer (71 kDa) in solution and in complex with CheW (18 kDa) and CF4Q (33 kDa) (Figure 2). We initially used the labeling reagent at a molar excess of 6 to label a 51 μM CheA solution and complexes having 51 μM protein in total. Under these reaction conditions, we found 62 labeled sites, which account for about 10% of the protein's structure. A comparison of the residue modification levels of the unbound CheA dimer versus the CheA dimer in complex reveals that many residues undergo decreases in labeling (Figure S1). Because vesicles and multiple proteins are present in the complex and could affect CheA reactivity with DEPC in unexpected ways, we felt that a simple comparison of labeling extents between unbound CheA and the complex would likely be insufficient to obtain definitive structural information. Consequently, we explored the effect of the vesicles on DEPC reactivity to ensure the vesicles themselves do not substantially hinder DEPC reactivity. In addition, we measured the labeling rates of CheA residues by reacting the protein and its complex with multiple DEPC concentrations as a way to account for the differences in protein content between the two samples.

DEPC Labeling of Peptides and CheA With and Without Vesicles

To study the effect of the vesicles on DEPC reactivity, the peptides bradykinin and angiotensin II were labeled by DEPC at three different concentrations in the presence or absence vesicles composed of 60% DOPC with 40% DGS-NTA(Ni^{2+}) (Figure 3a). Figure 3b shows that the modification profile of each peptide does not substantially change even when the vesicles are added at a concentration of 860 μM, indicating that the influence of vesicles on DEPC labeling is relatively minor.

We also used DEPC to label free CheA with and without 860 μM vesicles. Figure 4 shows that a majority (67%) of the residues do not undergo significant changes in labeling, suggesting that the presence of the vesicles does not have a major impact on DEPC reactivity. The 33% of the residues that do undergo statistically significant labeling changes may interact nonspecifically with the vesicles. Moreover, the vast majority of the residues that change in labeling are Ser, Thr, and Tyr residues, which have reactivity that is known to be very sensitive to changes in the local hydrophobic environment.[42–46] Despite some changes in labeling in the presence of vesicles, it is important to note that CheA does not interact directly with the vesicles in the chemoreceptor complex because of its location in the complex (Figure 2) and because the vesicle surface is largely covered by the bound receptor CF.

Author Manuscript Author Manuscript Author Manuscript Author Manuscript

DEPC Labeling of CheA in Solution vs. Complex at Different DEPC Concentrations

In addition to the effect of the vesicles, the other proteins in the chemoreceptor complex could affect DEPC's reactivity with CheA in a non-specific way. Indeed, recent DEPC labeling studies of antibody-antigen complexes indicate that the presence of other large proteins (e.g. antibodies) influence the DEPC labeling of antigen proteins via reaction competition.[31] To account for the presence of not only the vesicles but also these other proteins that react to different extents with DEPC, we measured the extent of residue labeling at different DEPC concentrations to obtain an effective labeling rate for individual residues. Changes in the effective labeling rate of a given CheA residue in complex, rather than the extent of labeling at a single DEPC concentration, would suggest a change in the solvent accessibility or microenvironment of that residue in the complex, with decreased labeling suggesting burial in the complex. To obtain more reliable quantitative information at the different DEPC concentrations, we used PRM measurements to simultaneously monitor the labeling rate of 20 residues. The 20 residues were chosen because they span each of the five domains in CheA. We also avoided choosing residues in CheA that showed a labeling change in the presence of vesicles alone (e.g. data in Figure 4).

From the labeling measurements at several different DEPC concentrations, we can obtain plots whose slopes are related to the labeling rate of each residue (Figure 5 and Figure S2). Twoway ANOVA tests were used to determine whether the estimated labeling rate of a given residue in CheA changed significantly upon complex formation. From these experiments, we find that five residues have decreased labeling upon complex formation, including Thr134/Ser136/Thr139 (these three residues cannot be resolved by MS/MS), Ser258, Tyr331 (Figure 5a), Ser381/His384, and His543. The labeling rates of 14 residues have no change as exemplified in Figure 5b, and one residue (His181, Figure 5c) has an increased labeling rate. These results are summarized in Table S1.

Comparison of CL-MS Data to Chemoreceptor Complex Model

CL-MS provides structural information about the molecular environment around residue side chains. When it comes to protein interactions, CL-MS measurements typically indicate binding sites when modification extents of given residues decrease upon protein complex formation, although increased labeling is sometimes observed and suggests a change in residue microenvironment. The core signaling unit complex of CheA with CheW and the CF4Q membrane receptor consists of a pair of trimers of receptor CF4Q dimers, two CheW molecules, and a CheA dimer (Figure 6).[36] Unbound CheA is also largely dimeric (93% dimer at 51 μM based on its Kd of 0.49 μM).[47]

The CL-MS data for the 20 labeled residues in CheA were compared to the chemoreceptor complex model. There is no complete crystal or NMR structure for the chemoreceptor complex, but a partial model has been built from structures of individual components and includes CheW, the cytoplasmic fragment (CF4Q, receptor), and the P3, P4, and P5 domains of the CheA dimer. This model was built based on an 8.4 Å resolution electron density map obtained by cryo-electron tomography of *in-vitro* signaling complexes of CF4Q, CheA, and CheW. Molecular dynamics flexible fitting was used to optimize the positions of crystal structures of homologous protein components to fit this electron density map, yielding a

Author Manuscript Author Manuscript Author Manuscript Author Manuscript

model (pdb 6s1k) of the signaling array containing the receptor fragment, CheW, and the P3, P4, and P5 domains of CheA.[37] The P1 and P2 domains of CheA, which are connected by flexible linkers to each other and to the rest of CheA (i.e. P3, P4, P5 domains), are not present in this structural model of the signaling complex.

We first considered the CL-MS results of 10 residues in the P3, P4, and P5 domains of CheA to assess the ability of CL-MS to provide accurate structural information for membrane-associated protein complexes. To facilitate comparisons of the CL-MS data (Figure S2) with the predicted protein-protein interfaces in the model, we conducted a PISA (Proteins, Interfaces, Structures and Assemblies) analysis of the complex,[48] allowing us to identify residues in CheA that are at an interface with CheW or CF4Q. Moreover, additional structural information in the model together with prior mutagenesis results, biochemical data, and MD simulations were considered to predict changes for other residues not found at interfaces. Table 1 summarizes the predicted and observed labeling changes upon comparing the unbound CheA dimer to CheA in complex. Overall, we find good agreement with the chemoreceptor complex model, as the majority (8/10) of the residues change as expected. For example, His300 sits at the end of a helix in the P3 domain and is quite exposed in both the CheA dimer and the chemoreceptor complex (Figure 7), so its reactivity is not expected to change, and indeed, it does not. In contrast, His543 is positioned at one of the interfaces between CheA and CheW (Figure 7), and therefore as expected, it undergoes a decrease in labeling. His384 (or possibly Ser381) also decreases in labeling extent, and even though MS/MS cannot definitively identify which residue is labeled, it is more likely to be His384, as His residues are more nucleophilic and thus more inherently reactive than Ser residues. Both Ser381 and His384 are near the ATP binding site,[49] and based on comparisons of the CheA dimer from *Thermatoga maritima* (PDB: 1B3Q)[50] and the chemoreceptor model complex (pdb 6s1k), His384 is predicted to become more buried, explaining its decreased labeling extent.

Tyr331 also decreases in labeling extent upon complex formation, and its reactivity is particularly interesting because MD calculations and mutagenesis experiments indicate that this residue undergoes a significant change in its microenvironment in the kinase-on complex. Tyr331 forms a hydrogen bond across the CheA dimer interface (P4 to P3'). HDX-MS results (Tran *et al.*, manuscript in preparation) indicate that the P3 dimer interface is stronger in CF4Q complexes, predicting a decrease in labeling of Tyr331. In addition, molecular dynamics simulations[51] and generalized simulated annealing[37] of the structural model of the complex suggest that CheA adopts two conformations, with P4 in an "undipped" (as shown in Figure 1) or "dipped" position (not shown), depending on the conformation of the connecting segment between P3 and P4, which are residues 320–332. Thus, it is likely that Tyr331, which is part of this connecting segment, undergoes a change in microenvironment when incorporated into the signaling complex, consistent with the observed change in labeling of this residue.

Two of the 10 residues (i.e. Tyr614 and Lys616) do not undergo the predicted labeling changes based on the PISA analysis, although in one case it is likely due to limitations of the structural model. Both residues participate in the CheA/CheW interface 1 of the model, according to the PISA analysis. Even though Lys616 is very solvent exposed in the model,

Author Manuscript Author Manuscript Author Manuscript Author Manuscript

a hydrogen bond between the sidechain nitrogen of Lys616 and a backbone carbonyl of Leu158 on CheW causes it to be categorized as an interface residue (Figure 8). The lack of a significant change in labeling of Lys616 upon formation of the complex suggests that this residue does not form the hydrogen bond to CheW that is suggested by the structural model. Moreover, it is important to note that the model does not include the final nine C-terminal residues after Leu158 that are naturally found in CheW, so the structure of this interface is likely incomplete.

The lack of a labeling change for Tyr614 is less definitive. This residue is predicted to be in a pocket near the CheA/CheW binding interface (Figure 8), but no change in labeling is observed. Previously, we found that weak nucleophilic residues, like Tyr, are labeled to a greater extent when they are in a “sweet spot” in which there are enough nearby hydrophobic sites and moderate solvent accessibility to increase the local concentration of DEPC.[42–46] It is possible that this residue has a higher SASA with less hydrophobic environment in the unbound form of CheA, and upon binding to CheW the SASA drops but a more hydrophobic environment is created. The net result would be a re-balancing of hydrophobicity and SASA that still allows the same amount of labeling. Of course, another explanation is that CL-MS data are not high enough quality or sensitive enough to detect a labeling change.

When considered as a whole, the CL-MS data for the 10 residues in the P3, P4, and P5 domains of CheA are mostly consistent with the model of the chemoreceptor complex, providing solid evidence that DEPC labeling can report on protein-protein interactions involving membrane-associated proteins. In light of these promising results, we next considered 10 more residues in the P1 and P2 domains that are not part of the structural model and for which there is no other definitive structural information in the chemoreceptor complex. These domains are thought to form an ensemble of structures below the complex formed between the CheA kinase core (P3, P4, P5 domains), CheW, and receptor.[52] Consistent with the expectation that these domains are not buried upon complex formation, labeling rates do not change significantly for seven of the 10 residues in the P1 and P2 domains and the flexible linkers (i.e. L1 and L2) that connect the domains (Table S1).

Decreased labeling is observed at two sites (Thr134/Ser136/Thr139 and Ser258) in linkers L1 and L2, suggesting that the linkers sample a different ensemble of structures in the complex that alters the environment of these residues. The MS/MS data do not allow unambiguous assignment of Thr134, Ser136, and/or Thr139 as the labeled site(s), but this region clearly undergoes a decrease in labeling (Figure S2). These residues are located near the edge of the P1 domain and are at the beginning of an unstructured linker that connects the P1 and P2 domain. This linker region is not expected to be buried upon complex formation, but evidently these residues experience a change in microenvironment upon complex formation. In previous work, it was shown that the reactivity of weakly nucleophilic residues such as Ser, Thr, and Tyr is increased when flanked by nearby hydrophobic groups,[42–46] so a decrease in labeling might indicate that these residues become even more exposed in the complex. Ser258, which is located in the flexible linker that connects the P2 and P3 domains, also may undergo a decrease in labeling for similar reasons.

Author Manuscript Author Manuscript Author Manuscript Author Manuscript

Interestingly, the only residue in all of CheA which shows *increased* labeling upon complex formation is His181 in the P2 domain. His181 is part of a helix near the site where CheA transiently binds the protein CheY (which is not present in this study) for phosphotransfer (Figure S3).[53] The increased labeling of His181 suggests that when CheA forms signaling complexes with CheW and receptor, the P2 domain of CheA becomes more accessible for CheY binding to enable phosphotransfer from CheA to CheY. Altogether, these CL-MS results provide new insights into the arrangement of these domains and linkers in the signaling complex that is unavailable from other methods.

Conclusions

In this work, DEPC-based CL-MS has been applied to study the protein-protein complex of a membrane-associated protein, which is a class of proteins that is difficult to investigate by other techniques. Using CheA as a model system, we find that DEPC labeling chemistry is not substantially altered by the presence of vesicles, despite its moderate hydrophobicity, allowing it to be used to study protein binding in the presence of artificial membranes. Comparing the DEPC labeling results of unbound CheA and CheA in its chemoreceptor complex required measurements of the effective DEPC labeling rate to account for the influence of the other proteins, CheW and CF4Q, on DEPC reactivity. Using PRM to maximize measurement precision, we determined the effective labeling rate of 20 residues in CheA, 10 of which are present in the CheA kinase core (P3, P4, P5 domains) that have a structural model for comparison and 10 of which are in the P1 and P2 domains that do not have definitive structural information. We find that the labeling results for the 10 residues in the CheA kinase core are mostly consistent with the structural model and other experimental information, providing validation of the CL-MS results. The CL-MS results for the 10 residues from the P1 and P2 domains yield new structural insight about these domains in the signaling complex that has resisted characterization by other methods. Overall, this study demonstrates the promise of DEPC-based CL-MS for studying the interactions of membrane-associated proteins. Future work will enhance the LC-MS/MS analyses of samples containing high concentrations of lipid vesicles to increase the number of residues that can be characterized at the same time, thereby improving the structural resolution of the technique. In addition, studies on more membrane proteins will be conducted to more fully assess the influence of artificial membranes on DEPC labeling.

Supplementary Material

Refer to Web version on PubMed Central for supplementary material.

Acknowledgements

This work was supported by the National Institutes of Health (NIH) under grants R01 GM075092, R35 GM145272 and R01 GM120195. The authors wish to thank the UMass Amherst Institute of Applied Life Sciences Mass Spectrometry Core Facility (RRID:SCR_019063) and Prof. Stephen J. Eyles and Prof. Cedric E. Bobst for their help with the Thermo Scientific Orbitrap Fusion Tribrid mass spectrometer. The Thermo Scientific Orbitrap Fusion Tribrid mass spectrometer was purchased with funds from the NIH grant S10OD010645. We also acknowledge Dr. Patanachai Kong Limpikirati for his advice on the PRM experiments and data analysis.

Author Manuscript Author Manuscript Author Manuscript Author Manuscript

References

1. Eyster KM, New paradigms in signal transduction. Biochem. Pharmacol 2007, 73 (10), 1511–1519. [PubMed: 17097069]
2. Rosenbaum DM; Rasmussen SGF; Kobilka BK, The structure and function of G-protein-coupled receptors. Nature 2009, 459 (7245), 356–363. [PubMed: 19458711]
3. Yin H; Flynn AD, Drugging Membrane Protein Interactions. Annu. Rev. Biomed. Eng 2016, 18, 51–76. [PubMed: 26863923]
4. Carpenter EP; Beis K; Cameron AD; Iwata S, Overcoming the challenges of membrane protein crystallography. Curr. Opin. Struct. Biol 2008, 18 (5), 581–586. [PubMed: 18674618]
5. Kang C; Li Q, Solution NMR study of integral membrane proteins. Curr. Opin. Chem. Biol 2011, 15 (4), 560–569. [PubMed: 21684799]
6. Majeed S; Ahmad AB; Sehar U; Georgieva ER, Lipid Membrane Mimetics in Functional and Structural Studies of Integral Membrane Proteins. Membranes 2021, 11 (9), 685. [PubMed: 34564502]
7. McPherson A, Introduction to protein crystallization. Methods 2004, 34 (3), 254–265. [PubMed: 15325645]
8. Thonghin N; Kargas V; Clews J; Ford RC, Cryo-electron microscopy of membrane proteins. Methods 2018, 147, 176–186. [PubMed: 29702228]
9. Liang B; Tamm LK, NMR as a tool to investigate the structure, dynamics and function of membrane proteins. Nat. Struct. Mol. Biol 2016, 23 (6), 468–474. [PubMed: 27273629]
10. Alcor D; Gouzer G; Triller A, Single-particle tracking methods for the study of membrane receptors dynamics. Eur. J. Neurosci 2009, 30 (6), 987–997. [PubMed: 19735284]
11. Christie S; Shi X; Smith AW, Resolving Membrane Protein–Protein Interactions in Live Cells with Pulsed Interleaved Excitation Fluorescence Cross-Correlation Spectroscopy. Acc. Chem. Res 2020, 53 (4), 792–799. [PubMed: 32227891]
12. García-Sáez AJ; Schwille P, Single molecule techniques for the study of membrane proteins. Appl. Microbiol. Biotechnol 2007, 76 (2), 257–266. [PubMed: 17497147]
13. Calabrese AN; Radford SE, Mass spectrometry-enabled structural biology of membrane proteins. Methods 2018, 147, 187–205. [PubMed: 29510247]
14. Reading E; Walton Troy A.; Liko I; Marty Michael T.; Laganowsky A; Rees Douglas C.; Robinson Carol V., The Effect of Detergent, Temperature, and Lipid on the Oligomeric State of MscL Constructs: Insights from Mass Spectrometry. Chem. Biol 2015, 22 (5), 593–603. [PubMed: 26000747]
15. Laganowsky A; Reading E; Allison TM; Ulmschneider MB; Degiacomi MT; Baldwin AJ; Robinson CV, Membrane proteins bind lipids selectively to modulate their structure and function. Nature 2014, 510 (7503), 172–175. [PubMed: 24899312]
16. Konijnenberg A; Yilmaz D; Ingólfsson HI; Dimitrova A; Marrink SJ; Li Z; Vénien-Bryan C; Sobott F; Koçer A, Global structural changes of an ion channel during its gating are followed by ion mobility mass spectrometry. Proc. Natl. Acad. Sci. U. S. A 2014, 111 (48), 17170–17175. [PubMed: 25404294]
17. Harvey SR; Liu Y; Liu W; Wysocki VH; Laganowsky A, Surface induced dissociation as a tool to study membrane protein complexes. Chem. Commun 2017, 53 (21), 3106–3109.
18. Hebling CM; Morgan CR; Stafford DW; Jorgenson JW; Rand KD; Engen JR, Conformational analysis of membrane proteins in phospholipid bilayer nanodiscs by hydrogen exchange mass spectrometry. Anal. Chem 2010, 82 (13), 5415–5419. [PubMed: 20518534]
19. Reading E; Hall Z; Martens C; Haghighi T; Findlay H; Ahdash Z; Politis A; Booth PJ, Interrogating Membrane Protein Conformational Dynamics within Native Lipid Compositions. Angew. Chem. Int. Ed. Engl 2017, 56 (49), 15654–15657. [PubMed: 29049865]
20. Vahidi S; Bi Y; Dunn SD; Konermann L, Load-dependent destabilization of the γ-rotor shaft in FOF1 ATP synthase revealed by hydrogen/deuterium-exchange mass spectrometry. Proc. Natl. Acad. Sci. U S A 2016, 113 (9), 2412–2417. [PubMed: 26884184]

Author Manuscript Author Manuscript Author Manuscript Author Manuscript

21. Komolov KE; Du Y; Duc NM; Betz RM; Rodrigues J; Leib RD; Patra D; Skiniotis G; Adams CM; Dror RO; Chung KY; Kobilka BK; Benovic JL, Structural and Functional Analysis of a β(2)-Adrenergic Receptor Complex with GRK5. Cell 2017, 169 (3), 407–421. [PubMed: 28431242]
22. Liu; Zhang H; Niedzwiedzki DM; Prado M; He G; Gross ML; Blankenship RE, Phycobilisomes Supply Excitations to Both Photosystems in a Megacomplex in Cyanobacteria. Science (New York, N.Y.) 2013, 342 (6162), 1104–1107. [PubMed: 24288334]
23. Pan X; Vachet RW, Membrane Protein Structures and Interactions from Covalent Labeling Coupled with Mass Spectrometry. Mass Spectrom. Rev 2022, 41 (1), 51–69. [PubMed: 33145813]
24. Xu G; Chance MR, Hydroxyl radical-mediated modification of proteins as probes for structural proteomics. Chemical Rev. 2007, 107 (8), 3514–3543.
25. Mendoza VL; Vachet RW, Probing protein structure by amino acid-specific covalent labeling and mass spectrometry. Mass Spectrom. Rev 2009, 28 (5), 785–815. [PubMed: 19016300]
26. Schmidt C; Macpherson JA; Lau AM; Tan KW; Fraternali F; Politis A, Surface Accessibility and Dynamics of Macromolecular Assemblies Probed by Covalent Labeling Mass Spectrometry and Integrative Modeling. Anal. Chem 2017, 89 (3), 1459–1468. [PubMed: 28208298]
27. Guo C; Cheng M; Li W; Gross ML, Diethylpyrocarbonate Footprints a Membrane Protein in Micelles. J. Am. Soc. Mass Spectrom 2021, 32 (11), 2636–2643. [PubMed: 34664961]
28. Mendoza VL; Antwi K; Barón-Rodríguez MA; Blanco C; Vachet RW, Structure of the Preamyloid Dimer of β−2-Microglobulin from Covalent Labeling and Mass Spectrometry. Biochemistry 2010, 49 (7), 1522–1532. [PubMed: 20088607]
29. Mendoza VL; Barón-Rodríguez MA; Blanco C; Vachet RW, Structural Insights into the Pre-Amyloid Tetramer of β−2-Microglobulin from Covalent Labeling and Mass Spectrometry. Biochemistry 2011, 50 (31), 6711–6722. [PubMed: 21718071]
30. Liu T; Marcinko TM; Kiefer PA; Vachet RW, Using Covalent Labeling and Mass Spectrometry To Study Protein Binding Sites of Amyloid Inhibiting Molecules. Anal. Chem 2017, 89 (21), 11583–11591. [PubMed: 29028328]
31. Tremblay CY; Kirsch ZJ; Vachet RW, Epitope Mapping with Diethylpyrocarbonate Covalent Labeling-Mass Spectrometry. Anal. Chem 2022, 94 (2), 1052–1059. [PubMed: 34932327]
32. Wildman SA; Crippen GM, Prediction of Physicochemical Parameters by Atomic Contributions. J. Chem. Inf. Comput. Sci 1999, 39 (5), 868–873.
33. National Center for Biotechnology Information (2022). PubChem Compound Summary for CID 3051, Diethyl pyrocarbonate. Retrieved March 17, 2022 from https://pubchem.ncbi.nlm.nih.gov/compound/Diethyl-pyrocarbonate.
34. Miles EW, Modification of histidyl residues in proteins by diethylpyrocarbonate. In Methods Enzymol, Academic Press: 1977; Vol. 47, pp 431–442. [PubMed: 22021]
35. Muok AR; Briegel A; Crane BR, Regulation of the chemotaxis histidine kinase CheA: A structural perspective. Biochim. Biophys. Acta Biomembr 2020, 1862 (1), 183030. [PubMed: 31374212]
36. Parkinson JS; Hazelbauer GL; Falke JJ, Signaling and sensory adaptation in Escherichia coli chemoreceptors: 2015 update. Trends Microbiol. 2015, 23 (5), 257–266. [PubMed: 25834953]
37. Cassidy CK; Himes BA; Sun D; Ma J; Zhao G; Parkinson JS; Stansfeld PJ; Luthey-Schulten Z; Zhang P, Structure and dynamics of the E. coli chemotaxis core signaling complex by cryo-electron tomography and molecular simulations. Commun. Biol 2020, 3 (1), 24. [PubMed: 31925330]
38. Shrout AL; Montefusco DJ; Weis RM, Template-Directed Assembly of Receptor Signaling Complexes. Biochemistry 2003, 42 (46), 13379–13385. [PubMed: 14621982]
39. Li X; Eyles SJ; Thompson LK, Hydrogen exchange of chemoreceptors in functional complexes suggests protein stabilization mediates long-range allosteric coupling. J. Biol. Chem 2019, 294 (44), 16062–16079. [PubMed: 31506298]
40. Pan X; Limpikirati P; Chen H; Liu T; Vachet RW, Higher-Order Structure Influences the Kinetics of Diethylpyrocarbonate Covalent Labeling of Proteins. J. Am. Soc. Mass Spectrom 2020, 31 (3), 658–665. [PubMed: 32013423]
41. Zhou Y; Vachet RW, Diethylpyrocarbonate labeling for the structural analysis of proteins: label scrambling in solution and how to avoid it. J. Am. Soc. Mass Spectrom 2012, 23 (5), 899–907. [PubMed: 22351293]

Author Manuscript Author Manuscript Author Manuscript Author Manuscript

42. Limpikirati P; Hale JE; Hazelbaker M; Huang Y; Jia Z; Yazdani M; Graban EM; Vaughan RC; Vachet RW, Covalent labeling and mass spectrometry reveal subtle higher order structural changes for antibody therapeutics. MAbs 2019, 11 (3), 463–476. [PubMed: 30636503]
43. Limpikirati P; Pan X; Vachet RW, Covalent Labeling with Diethylpyrocarbonate: Sensitive to the Residue Microenvironment, Providing Improved Analysis of Protein Higher Order Structure by Mass Spectrometry. Anal. Chem 2019, 91 (13), 8516–8523. [PubMed: 31150223]
44. Tremblay CY; Limpikirati P; Vachet RW, Complementary Structural Information for Stressed Antibodies from Hydrogen–Deuterium Exchange and Covalent Labeling Mass Spectrometry. J. Am. Soc. Mass Spectrom 2021, 32 (5), 1237–1248. [PubMed: 33886284]
45. Biehn SE; Limpikirati P; Vachet RW; Lindert S, Utilization of Hydrophobic Microenvironment Sensitivity in Diethylpyrocarbonate Labeling for Protein Structure Prediction. Anal. Chem 2021, 93 (23), 8188–8195. [PubMed: 34061512]
46. Biehn SE; Picarello DM; Pan X; Vachet RW; Lindert S, Accounting for Neighboring Residue Hydrophobicity in Diethylpyrocarbonate Labeling Mass Spectrometry Improves Rosetta Protein Structure Prediction. J. Am. Soc. Mass Spectrom 2022, 33 (3), 584–591. [PubMed: 35147431]
47. Kott L; Braswell EH; Shrout AL; Weis RM, Distributed subunit interactions in CheA contribute to dimer stability: a sedimentation equilibrium study. Biochim. Biophys. Acta - Proteins and Proteom 2004, 1696 (1), 131–140.
48. Krissinel E; Henrick K, Inference of macromolecular assemblies from crystalline state. J. Mol. Bio 2007, 372 (3), 774–97. [PubMed: 17681537]
49. Hirschman A; Boukhvalova M; VanBruggen R; Wolfe AJ; Stewart RC, Active Site Mutations in CheA, the Signal-Transducing Protein Kinase of the Chemotaxis System in Escherichia coli. Biochemistry 2001, 40 (46), 13876–13887. [PubMed: 11705377]
50. Bilwes AM; Alex LA; Crane BR; Simon MI, Structure of CheA, a signal-transducing histidine kinase. Cell 1999, 96 (1), 131–41. [PubMed: 9989504]
51. Cassidy CK; Himes BA; Alvarez FJ; Ma J; Zhao G; Perilla JR; Schulten K; Zhang P, CryoEM and computer simulations reveal a novel kinase conformational switch in bacterial chemotaxis signaling. eLife 2015, 4, e08419. [PubMed: 26583751]
52. Briegel A; Ames P; Gumbart JC; Oikonomou CM; Parkinson JS; Jensen GJ, The mobility of two kinase domains in the Escherichia coli chemoreceptor array varies with signalling state. Mol. Microbiol 2013, 89 (5), 831–41. [PubMed: 23802570]
53. Mo G; Zhou H; Kawamura T; Dahlquist FW, Solution Structure of a Complex of the Histidine Autokinase CheA with Its Substrate CheY. Biochemistry 2012, 51 (18), 3786–3798. [PubMed: 22494339]

Author Manuscript Author Manuscript Author Manuscript Author Manuscript

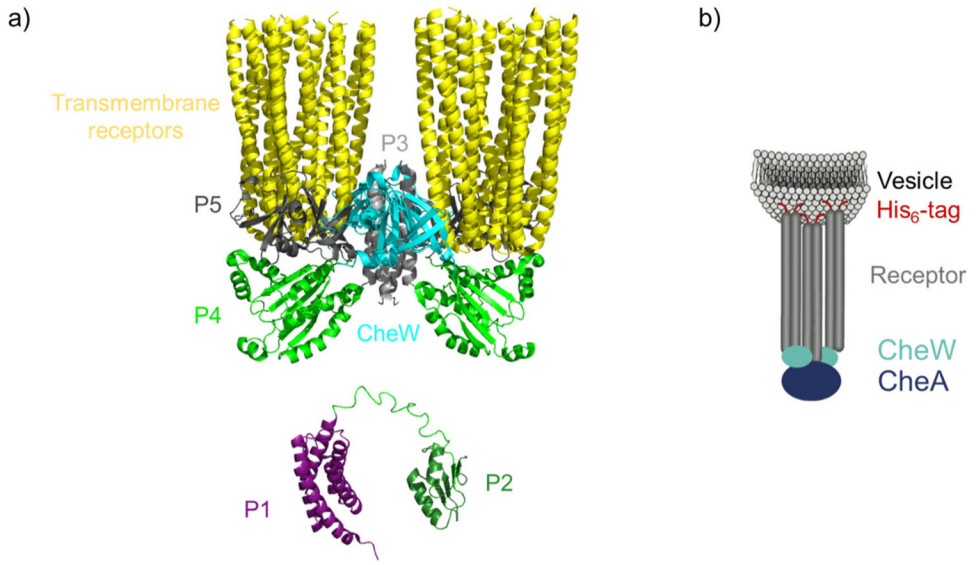

Figure 1:

a) Structural model of the chemotaxis histidine kinase (CheA) in complex with CheW and the transmembrane receptors. The receptors (yellow) extend upward toward the membrane; structures of the P3, P4, and P5 domains with CheW and transmembrane receptors are from electron microscopy measurements (PDB: 6S1K). The structures of the P1 and P2 domains are from separate nuclear magnetic resonance (NMR) measurements (PDB: 2LP4), and these domains are connected by an unstructured linker (not shown) to P3. b) Scheme of CheA in the membrane complex system containing CheW, the cytoplasmic fragment (CF4Q, receptor) and unilamellar vesicles that contain a Ninitrilotriacetic acid complex that anchors CF4Q to the vesicles via a His tag.

Author Manuscript Author Manuscript Author Manuscript Author Manuscript

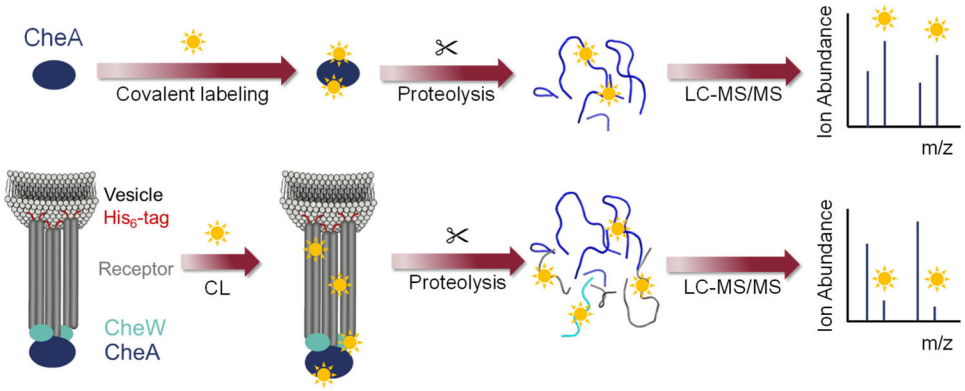

Figure 2:
Experimental workflow of DEPC CL-MS of unbound CheA and CheA in complex.

Author Manuscript Author Manuscript Author Manuscript Author Manuscript

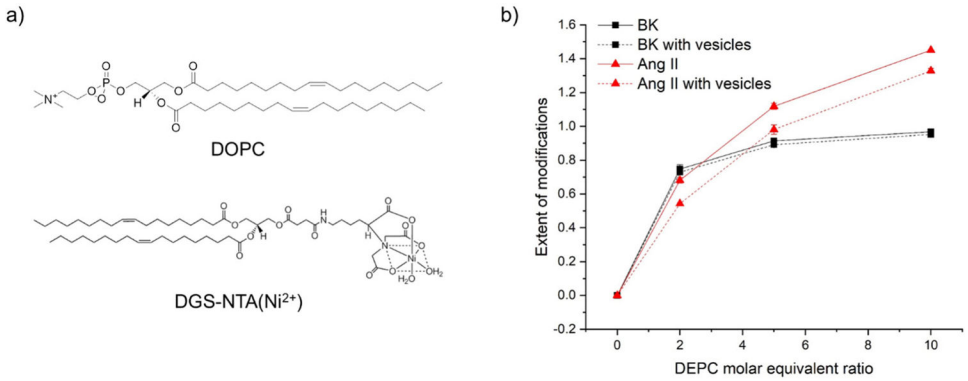

Figure 3:

a) Chemical structure of the lipids that comprise the vesicles. b) Modification extent of bradykinin (BK) and angiotensin II (Ang II) without and with vesicles (860 μM). The error bars represent the standard deviations from three replicate measurements.

Author Manuscript Author Manuscript Author Manuscript Author Manuscript

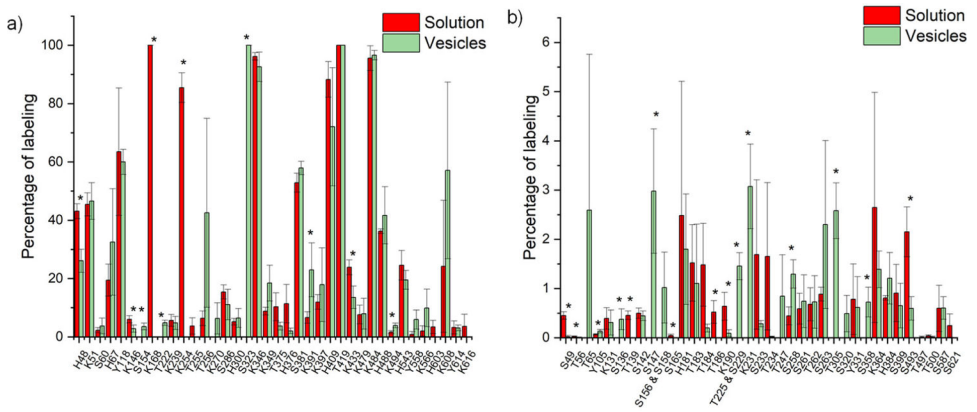

Figure 4:

DEPC labeling results for CheA in solution and in the presence of 860 μM vesicles. (a) Residues with average labeling percentages above 3%. (b) Residues with average labeling percentages below 3%. The protein was present at a concentration of 51 μM, and the DEPC concentration was 408 μM. The error bars are standard deviations from three replicate measurements. Asterisks indicate modified residues that undergo significant labeling changes in the presence of the vesicles based on student t-test with 95% confidence interval. The majority of the CheA residues do not undergo any significant change in labeling.

Author Manuscript Author Manuscript Author Manuscript Author Manuscript

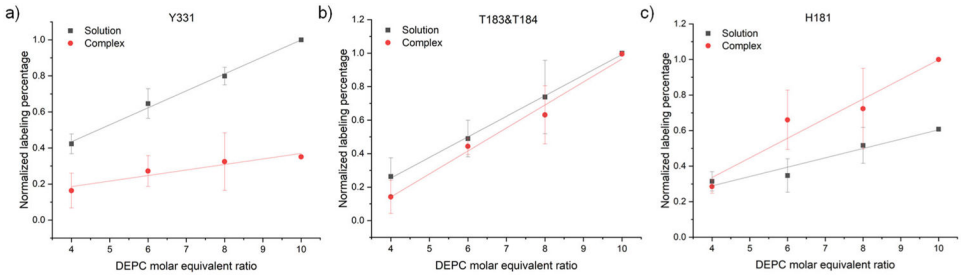

Figure 5:

Example plots of residue labeling percentages for CheA in solution without vesicles and in complex at different DEPC molar equivalents, as measured by PRM. Changes in the slopes of these plots indicate changes in residue reactivity in going from unbound CheA to CheA in complex. These plots can indicate (a) decreases in labeling, (b) no change in labeling, and (c) increases in labeling upon formation of the chemoreceptor complex. The error bars are standard deviations from five replicate measurements.

Author Manuscript Author Manuscript Author Manuscript Author Manuscript

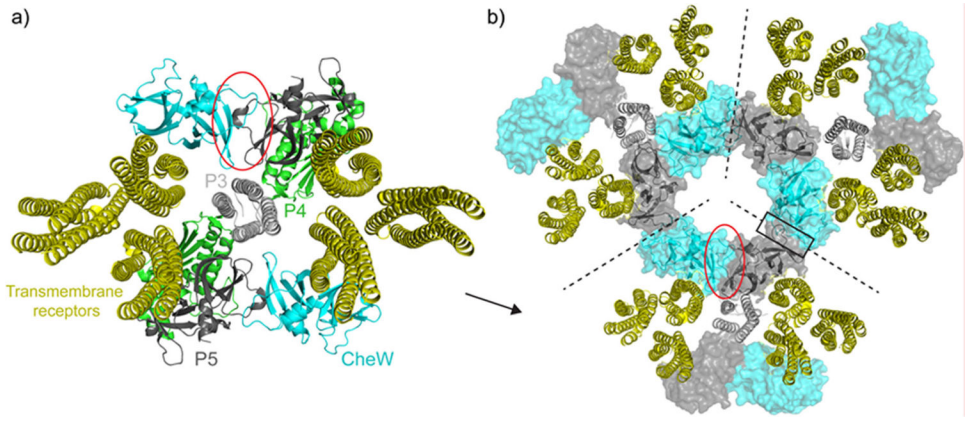

Figure 6:

Organization of kinase core (P3P4P5) in signaling complexes with CheW and CF4Q. Core signaling units (a, 6S1K) contain CheA/CheW interface 1 (red oval) and assemble into hexagonal arrays (b) via CheA/CheW interface 2 (black box). P4 domain is not shown in array model for clarity. Dashed lines divide the hexagon into three core signaling units.

Author Manuscript Author Manuscript Author Manuscript Author Manuscript

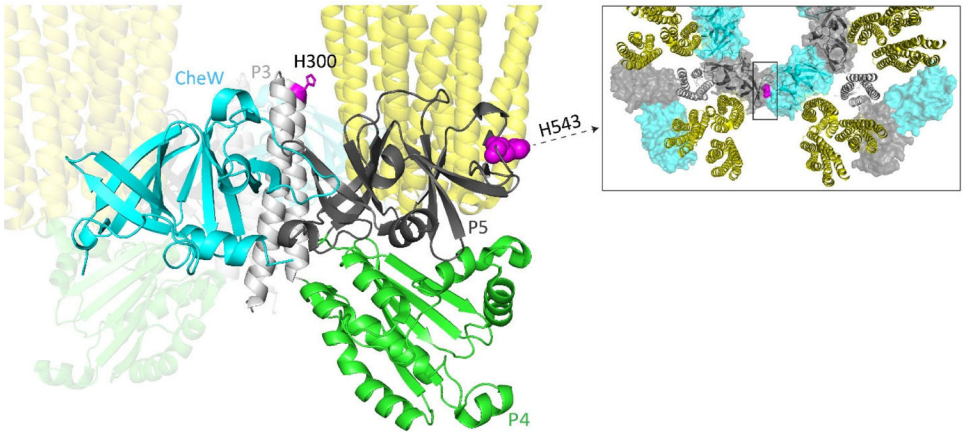

Figure 7:

Position of CheA residues His300 and His543 in complex. His300 (magenta sticks) is located at the end of a helix in the P3 domain (gray). His543 (magenta spheres) is located on the P5 domain (dark gray) at the interface with a neighboring CheW of the signaling array (black box highlights interface 2, inset).

Author Manuscript Author Manuscript Author Manuscript Author Manuscript

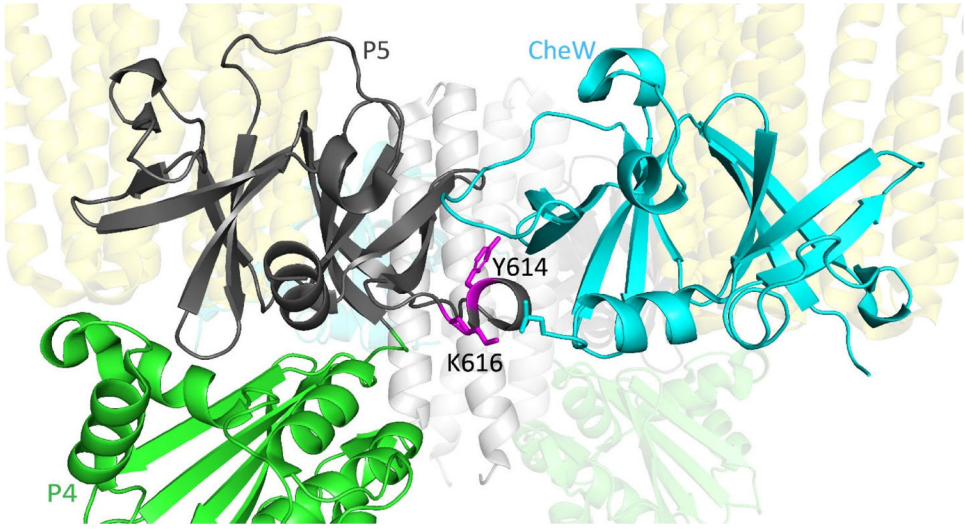

Figure 8:

CheA P5 interface with CheW. Tyr614 and Lys616 (magenta sticks) on the P5 domain of CheA (dark gray). In the structural model of the complex pdb:6S1K, Lys616 hydrogen bonds with Leu158 (cyan stick) on CheW (cyan).

Author Manuscript Author Manuscript Author Manuscript Author Manuscript

Table 1:

Summary of PISA predicted and experimentally observed CL-MS changes for residues in the P3, P4, and P5 domains of CheA.

Residue	Predicted labeling change (interface location)[1]	Observed labeling change
His300	None	None
Tyr331	Change[2] (CheA dimer interface)	Decrease
Thr375/His376[3]	None	None
Ser381/His384[3]	Decrease[4]	Decrease
Ser399	None	None
Lys479	None	None
His488	None	None
His543	Decrease (interface 2 with CheW)	Decrease
Tyr614	Decrease (interface 1 with CheW)	None
Lys616	Decrease (interface 1 with CheW)	None

[1] Predictions are largely based on PISA analysis of the structural model to identify residues present at a new interface in the complex. See text for details.

[2] Tyr331 is in the P3–4 connecting segment which is thought to be repositioned upon kinase activation, and thus is likely repositioned in the kinase-on complexes studied here.

[3] The MS/MS data are not definitive enough to allow the exact labeled residue to be identified in peptides containing these residues.

[4] These residues are in the ATP binding site. His384 changes positions in the complex, making it less exposed.